A Novel AlGaN/GaN MIS-HEMT with Enhanced Breakdown Voltage and Reduced Interface Trap Density

Chao Yang, Xiaorong Luo*, T. Sun, A. Zhang, D. Ouyang, S. Deng, J. Wei, and Bo Zhang

State Key Laboratory of Electronic Thin Films and Integrated Devices, School of Electronic Science and Engineering, University of Electronic Science and Technology of China, Chengdu, China
Email: xrluo@uestc.edu.cn, Tel: +86 28 83206788, Fax: +86 28 83207120

Keywords: MIS-HEMT, interfacial layer, channel modulated structure, interface trap density, breakdown voltage

Abstract

We proposed a novel AlGaN/GaN metal-insulator-semiconductor high-electron mobility transistor (MIS-HEMT) with AlN interfacial layer (*IL*) and channel modulated (*CM*) structure (*IL-CM-HEMT*). The AlN interfacial layer protects the etched interface from the degradation during the following high-temperature low pressure chemical vapor deposition (LPCVD) Si_3N_4 process (e.g. 780 °C) and reduces the interface trap density (D_{it}) effectively. With the interfacial layer, one order of reduction in D_{it} from the range 10^{13} to the range of ~10^{12}-10^{13} eV^{-1} cm^{-2}. In addition, the channel modulated structure as a novel termination technique is used to increase the breakdown voltage (*BV*). The *BV* of the proposed device was 412 V while that of the conventional device was 252 V.

INTRODUCTION

AlGaN/GaN high electron mobility transistor (HEMT) is indispensable for high efficiency and high-voltage power switching applications [1, 2]. Especially, the breakdown voltage (*BV*) is one of the most important properties in order to provide reliable performances at high power operations [3]. The electric field (E-field) crowding at the gate edge causes premature breakdown, which limits the applied range of AlGaN/GaN HEMTs. In consequence, it is necessary to employ the new techniques to improve the *BV*.

The metal-insulator-semiconductor (MIS) HEMTs with partially or fully recessed gate are considered an effective method to achieve normally-off operation [4]. The gate recess process causes plasma damage creating high density of interface traps and degrading the channel mobility [5]. Si_3N_4 deposited with low pressure chemical vapor deposition (LPCVD) as gate dielectric has shown superior performance [6]. However, the etched interface with weakened chemical bonds experiences stronger Ga and N out-diffusion in high-temperature LPCVD process (e.g. 780 °C), and suffers from significant degradation. Therefore, the interface protection engineering is required to modify the defect states.

In this work, we propose and experimentally demonstrate a normally-off high voltage MIS-HEMT, as shown in Fig. 1,

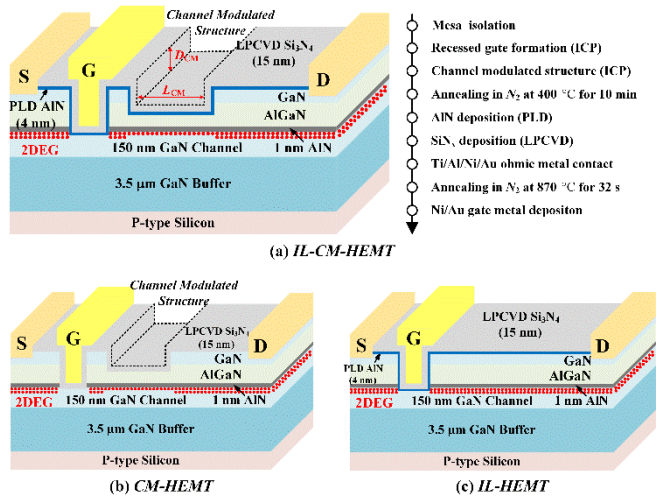

Fig. 1. Three-dimensional schematic of (a) *IL-CM-HEMT* and main fabrication process, (b) *CM-HEMT* and (c) *IL-HEMT*.

which features pulsed laser deposited (PLD) AlN interfacial layer (*IL*) and channel modulated (*CM*) structure (*IL-CM-HEMT*). The interfacial layer protects the etched interface from the degradation during the following high-temperature LPCVD Si_3N_4 process and reduces the interface trap density (D_{it}) effectively. The channel modulated structure as a novel termination technique is used to increase the *BV*.

DEVICE FABRICATION

The epitaxial AlGaN/GaN heterostructure used for fabricating the *IL-CM-HEMTs* was grown on 6-in (111) silicon substrate by metal organic chemical vapor deposition (MOCVD). The epitaxial layers consist of 2 nm GaN cap, 23 nm AlGaN barrier, 1 nm AlN interlayer, 300 nm GaN channel, and 3.5 μm GaN buffer. The Hall Effect measured density and mobility of the 2DEG were 9.5×10^{12} cm^{-2} and 1500 $cm^2/V\cdot s$, respectively. The proposed *IL-CM-HEMT* started with mesa isolation which was implemented by a high power Cl_2/BCl_3-based inductively coupled plasma (ICP) etching. Then the recessed gate and channel modulated structure are formed with low-power (e.g. ICP Power: 50 W) ICP etching by using AZ5214 photoresist as etching Mask. The depth of the recessed gate and channel modulated

structure is 27.5 nm and 14 nm, as confirmed by AFM measurements in Fig. 2. Then the wafers were treated by tetramethylammonium hydroxide (TMAH) solution at 85 ºC for 30 min to remove the post-etching residues and to modify the trench sidewall. The device was annealed at 400 °C for 10 min in N_2 ambient. Next, a 4 nm AlN layer by PLD was applied to protect the etched region surface from degradation, followed by a 15 nm LPCVD Si_3N_4 as the gate dielectric layer. After that, the Ti/Al/Ni/Au (22/140/55/45 nm) ohmic contact was deposited and annealed at 870 ºC for 32 s in N_2 ambient, with a contact resistance of 1.1 Ω·mm. Finally, Ni/Au (50/150 nm) metal gate was deposited to complete the fabrication flow. All three devices feature a gate length L_G of 1.5 μm, a gate-source distance L_{GS} of 1.5 μm, a gate-drain distance L_{GD} of 5 μm.

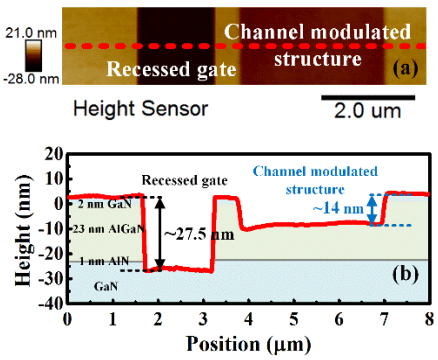

Fig. 2. (a) AFM morphology of the recessed gate and channel modulated structure and (b) Trenches profile along the dashed line before AlN and Si_3N_4 deposition.

EXPERIMENT RESULT

Fig. 3 is the high resolution cross section transmission electron microscope (TEM) micrographs of LPCVD-Si_3N_4/GaN MIS-structures (a) with and (b) without AlN interfacial layer. In order to avoid the interface degradation, an interface protection engineering was employed by inserting a thin AlN deposited by PLD between the Si_3N_4 and the etched-GaN surface. Fig. 3 (c) and Fig. 3 (d) show the surface morphology of the MIS-structures. The root-mean-square (RMS) roughness of the MIS-structures with AlN interfacial layer decreases to 0.284 nm from 0.454 nm of the MIS-structures without AlN interfacial layer.

In Fig. 4, the field effect mobility ($_{FE}$) is extracted by using long channel MIS-HEMTs with L_G/W_G=44/100 m. The increased RMS roughness would significantly decrease the 2DEG channel electron mobility, therefore the maximum field-effect mobility of the MIS-HEMT with AlN interfacial layer at V_{DS}=0.1 V increases to 208 $cm^2/V\cdot s$ from 95 $cm^2/V\cdot s$ of the MIS-HEMT without AlN interfacial layer.

Fig. 5 illuminates measured frequency-dependent *C-V* characteristics of circular MIS-diodes. The improved interface quality was verified by the reduced frequency dispersion from the frequency-dependent *C–V* characteristics of MIS-diode with AlN interfacial layer, compared with that of diode without AlN interfacial layer.

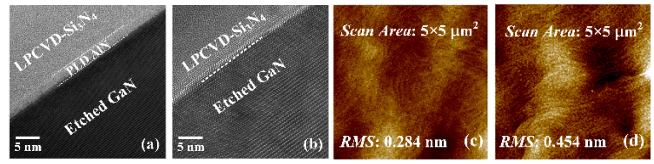

Fig. 3. HR-TEM micrographs of LPCVD-Si3N4/GaN MIS-structures (a) w/ and (b) w/o interfacial layer. Surface morphology (c) w/ and (b) w/o interfacial layer.

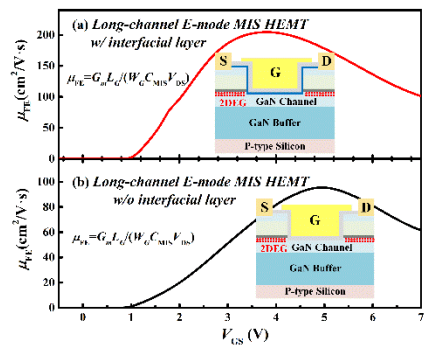

Fig. 4. Extracted field effect mobility ($_{FE}$) using long channel MIS-HEMTs.

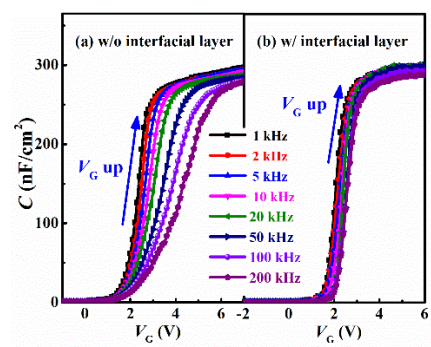

Fig. 5. Measured frequency dependent *C-V* characteristics of circular MIS-diodes (a) w/o and (b) w/ interfacial layer.

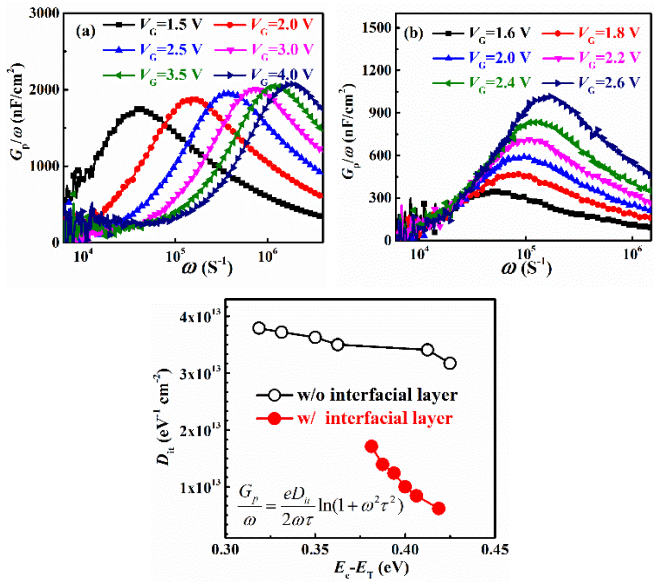

Fig. 6. Measured G_p/ω-f characteristics of circular MIS-diodes (a) w/o and (b) w/ AlN interfacial layer. (c) D_{it}-E_T mapping of MIS diodes using conductance method.

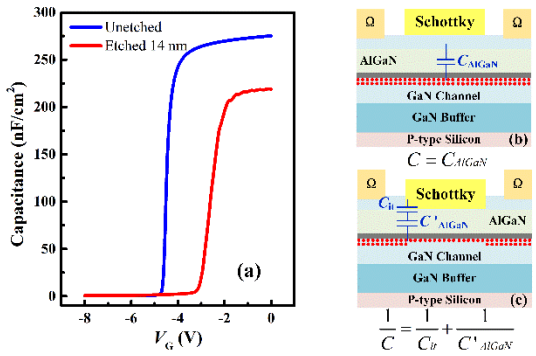

Fig. 7. (a) Measured C-V characteristics of circular Schottky diodes. Capacitance: (b) Unethed and (c) Etched schottky diodes.

In Fig. 6, conductance method was employed to map the D_{it}, with the cross sections of traps is 1×10^{-14} cm^{-2}. With the AlN interfacial layer, one order of reduction in D_{it} from the range 10^{13} to the range of ~10^{12}-10^{13} eV^{-1} cm^{-2} has been observed. In Fig. 7 (a), the electron density, calculated from the measured C-V characteristics, is 9.5×10^{12} cm^{-2} (Unetched line) and 2.1×10^{12} cm^{-2} (Etched line), respectively. The interface traps, caused by etched process, would introduce an additional capacitance (C_{it}), which decreases the total capacitance, as shown in Fig. 7 (b) and Fig. 7 (c).

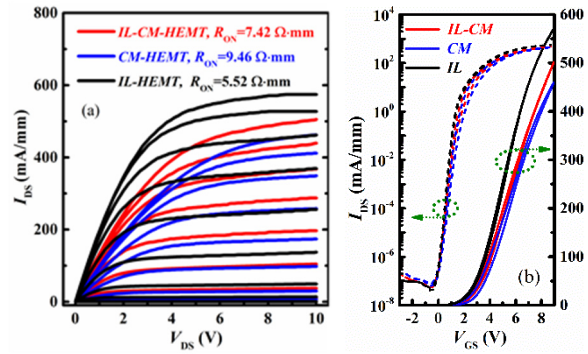

Fig. 8. Measured (a) I-V output characteristics for three kinds of devices. (b) Transfer and I-V hysteresis loop characteristics.

Fig. 8 illuminates the measured I-V output characteristics and transfer hysteresis loop characteristics. Compared with the *IL-HEMT*, the *IL-CM-HEMT* shows a slight decrease in the I_{DS}, because the *CM* structure decreases the 2DEG density. Owing to the reduced interface trap density by interfacial layer, *IL-CM-HEMT* obtains a higher I_{DS} than those of *CM-HEMT* and a decreased current hysteresis phenomenon appears in *IL-HEMT* and *IL-CM-HEMT*.

Fig.9 indicates the measured I-V characteristics and simulated surface E-field distributions on the blocking state. The BV are 412 V, 403 V and 252 V for three kinds of devices, respectively. The channel modulated structure as a termination technique reduces the E-field peak at the gate edge and causes a new E-field peak at the end of channel modulated structure, as shown in Fig. 10, which achieves more uniform surface E-field distribution and higher average E-field strength, and thus realizing an improved BV.

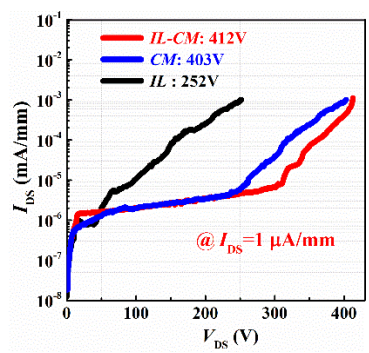

Fig. 9. Measured off-state breakdown characteristics at I_{DS}=1 A/mm.

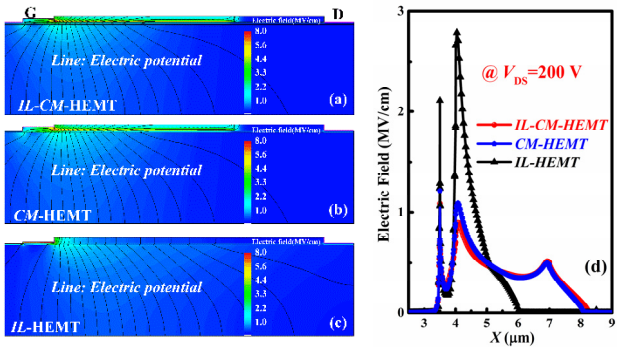

Fig. 10. Simulated surface E-field distributions at V_{DS}=200 V.

TABLE I. PHYSICAL PROPERTIES OF GAN AND ALN IN THE SIMULATION.

Material	GaN	AlN
$\mu_{e,max}(cm^2/Vs)$	1500	300
$\mu_h(cm^2/Vs)$	22	14
$v_s(10^7 cm/s)$	2.5	2.2
Band-offsets	$0.7\times(E_g(Al_xGa_{1-x}N)-E_g(GaN))$	

The physical mechanism is analyzed based on 2D Sentaurus TCAD from Synopsys. Several important physical effects such as bandgap narrowing, variable effective mass, doping dependent mobility at high electric fields and spontaneous polarizations are accounted in simulations. Table 1 shows some physical properties of GaN and AlN. The physical properties of the $Al_xGa_{1-x}N$ in simulation are calculated from GaN (x=0) and AlN (x=1) nonlinearly.

CONCLUSIONS

In conclusion, we propose a novel normally-off AlGaN/GaN MIS-HEMT, which features AlN interfacial layer and channel modulated structure. The AlN interfacial layer could improve interface quality and reduce interface trap density, thus a high channel effective mobility and low dynamic on-resistance degradation are both achieved by the advanced device structure and fabrication process. The channel modulated structure modulates the E-filed distribution and spreads the depletion region, thus *BV* is drastically improved by 63% in comparison with the MIS HEMT without channel modulated structure.

ACKNOWLEDGEMENTS

This work was supported in part by the National Natural Science Foundation of China under Grant 51677021, and in part by the National Natural Science Foundation of China under Grant 61874149.

REFERENCES

[1] U. K. Mishra, et al., *AlGaN/GaN HEMTs—An overview of device operation and application*, Proc. IEEE, Vol. 90, pp. 1022–1031 (2002).

[2] B. Song, et al., *Effect of Fringing Capacitances on the RF Performance of GaN HEMTs With T-Gates*, IEEE Trans. Electron Devices, Vol. 61, pp. 747-754 (2014).

[3] M. Kim, et al., *High Breakdown Voltage AlGaN/GaN HEMTs Employing Recessed Gate Edge Structure*, 2010 CS MANTECH conference, pp. 237-240, May 2010.

[4] T. Oka, et al., *AlGaN/GaN Recessed MIS-Gate HFET With High-Threshold-Voltage Normally-Off Operation for Power Electronics Applications*, IEEE Elect. Devi. Lett., Vol. 29, pp. 668-670 (2008).

[5] B. Lu, et al., *An Etch-Stop Barrier Structure for GaN High-Electron-Mobility Transistors*, IEEE Elect. Devi. Lett., Vol. 34, pp. 369-371 (2013).

[6] M. Hua, et al., *Integration of LPCVD-SiN_x Gate Dielectric with Recessed-gate E-mode GaN MIS-FETs: Toward High Performance, High Stability and Long TDDB Lifetime*, *2016 IEEE Electron Devices Meeting (IEDM)*, p. 10.4.1-10.4.4, Dec 2016.

ACRONYMS

MIS: Metal-Insulator-Semiconductor
HEMT: High-Electron Mobility Transistor
LPCVD: Low Pressure Chemical Vapor Deposition
PLD: Pulsed Laser Deposition
MOCVD: Metal Organic Chemical Vapor Deposition
2DEG: Two-Dimensional Electron Gas
ICP: Inductively Coupled Plasma
AFM: Atomic Force Microscope
HR-TEM: High-Resolution Transmission Electron Microscope